SCIENTIFIC Publishing Limited

3D Printing Innovations

https://ojs.ukscip.com/index.php/3dpi

Review

The Vascularization Crisis in 3D Bioprinting: Channel Engineering, Anastomosis, and the Missing Bridge to In Vivo Perfusion

Ignatius Echezona Ekengwu [1,*], Damian Chigozie Anyadike [1], Anthonia Ekene Ilechukwu [1] and Swift Onyegirim [2]

[1] Department of Mechanical Engineering, Nnamdi Azikiwe University, Awka 420007, Nigeria

[2] Department of Mechanical Engineering, Chukwuemeka Odumegwu Ojukwu University, Uli 431124, Nigeria

[*] Correspondence: ie.ekengwu@unizik.edu.ng

Received: 27 September 2025; **Revised:** 12 November 2025; **Accepted:** 16 November 2025; **Published:** 12 December 2025

Abstract: Fabricating living tissues thick enough to sustain organ-level function requires a functional vascular supply, as cells beyond approximately 200 μm from a nutrient source cannot maintain aerobic metabolism regardless of architectural refinement. This review examines the vascularization challenge in 3D bioprinting through the lens of engineering failure analysis, identifying the specific barriers preventing in vitro success from translating to in vivo function. Three interlocking challenges are systematically addressed: fabricating hierarchically organized channels spanning the full vascular tree from millimetre-scale trunks to sub-100 μm capillary beds; the range of anastomotic strategies researchers are pursuing to connect printed channels with host circulation; and the persistent, poorly explained failure of constructs that perform well in bioreactors to maintain perfusion after implantation. Drawing on mechanistic evidence from materials science, vascular biology, and surgical literature, four root causes of in vivo failure are identified: stiffness mismatch between printed and native vessel walls; temporal mismatch between hydrogel degradation and angiogenic invasion; the near-universal omission of pericyte support from bioprinted endothelial networks; and immunological assault on allogeneic endothelial linings inadequately shielded by current bioinks. None of these failure modes is inevitable, yet none will be resolved through printing technology alone. Progress requires simultaneous advances in bioink mechanobiology, co-culture vascular biology, bioreactor conditioning, and shared performance benchmarks that the field currently lacks. A structured three-phase translational roadmap organized around objectively measurable milestones is proposed to focus research effort on the specific barriers that current evidence identifies as rate-limiting.

Keywords: 3D Bioprinting; Vascularization; Hierarchical Channel Engineering; Anastomosis; In Vivo Perfusion; Bioink; Pericyte; Compliance Mismatch

1. Introduction

Walk into any hospital treating patients with end-stage organ failure and the arithmetic of the problem becomes stark. Globally, hundreds of thousands of people are waiting for a kidney, a liver, a heart—organs that the body can no longer provide but that medicine cannot yet reliably manufacture. Regenerative medicine promised, decades ago, that tissue engineering would close that gap [1]. To an extent, it has. Skin grafts, tracheal cartilage, bladder scaffolds [2], corneal patches—these achievements are real and they save lives. But the organs that kill most people in the transplant queue, the solid parenchymal organs whose metabolic demands are vast, have remained stubbornly out of reach. The reason is not lack of effort or ingenuity. It is a physical problem: blood.

Every cell in the liver, kidney, heart, or pancreas sits within roughly 200 µm of a capillary. Not by coincidence—by evolutionary necessity. Oxygen diffuses through tissue at a rate governed by simple physics, and beyond that distance, the partial pressure drops below what mitochondria require. In the natural organ, this proximity is achieved by a vascular tree of extraordinary structural complexity, spanning four orders of magnitude from the aorta to the capillary wall. Engineers have known this constraint for decades. The question that has driven—and continues to frustrate—tissue engineering research is deceptively simple: how do you reproduce that tree inside a fabricated construct, at sufficient resolution, within a biocompatible matrix, while keeping the cells alive?

Three-dimensional bioprinting entered this debate with genuine transformative potential [3–5]. By precisely depositing cell-laden hydrogels layer by layer, or extruding living inks through nozzles calibrated to the micrometre [6,7], bioprinting offered something earlier scaffold techniques could not: spatial control. If you could print a channel where you wanted it, at the diameter you needed, lined with the cells that maintain patency, you might, finally, build a perfusable tissue. And indeed, the last decade has produced results that would have seemed like science fiction to the founders of tissue engineering. Researchers have printed functional cardiac patches [8, 9], vascularized liver lobule analogues [10, 11], perfused kidney tubule chips [12], bionic ears and bone-mimicking constructs [13, 14], and, most dramatically, a near-anatomically faithful human heart from collagen bioink. Publications have multiplied, venture capital has followed, and regulatory agencies have begun drafting frameworks for bioprinted products.

Yet here is the uncomfortable truth that motivates this review: none of those constructs has been implanted into a human being and sustained physiological organ function by integrating with the patient's own vasculature. The bioprinted heart printed by Lee and colleagues in 2019 [15]—a landmark result by any measure—lacked contractile cells of sufficient maturity and had no functional coronary circulation. The vascularized constructs that survive weeks in bioreactor culture frequently show channel collapse, endothelial regression, or thrombosis within days of animal implantation. The field has accumulated substantial evidence of in vitro feasibility; sustained in vivo durability remains to be demonstrated at therapeutic scale. That gap, between bioreactor success and in vivo function, is what we have chosen to call the vascularization crisis, and it is the subject of this paper.

We should be clear about what this review is and what it is not. It is not a catalogue of every vascularization method described in the literature; several excellent systematic reviews already serve that purpose. Rather, it is a critical mechanical dissection of why the problem remains unsolved and what, specifically, concretely, would need to change for it to be solved. We examine hierarchical channel engineering from a fabrication physics perspective, anastomosis strategies from a vascular biology perspective, and in vivo failure from a combined materials-immunology perspective. We write as mechanical engineers who work at the intersection of bioprinting and vascular biology, and we have tried to bring to this review the same rigour we would apply to any engineering failure analysis. When a bridge collapses, engineers do not stop at noting that it failed; they trace the mechanism. We intend to do the same for the bioprinted vascular construct.

Literature for this review was identified through structured searches of PubMed, Web of Science, and Scopus using the terms "3D bioprinting vascularization," "bioprinted vascular constructs," "hierarchical channel engineering," "anastomosis tissue engineering," and "in vivo perfusion bioprinting," applied individually and in combination. The search covered publications from 1993 through December 2024, with priority given to studies published from 2012 onward to capture the contemporary bioprinting era. Inclusion required direct relevance to vascular channel fabrication, anastomosis, or in vivo perfusion; peer-reviewed English-language publication; and, wherever possible, quantitative performance data. Conference abstracts and preprints were excluded. Reference lists of key included articles were screened manually for additional sources. Studies reporting both negative and positive outcomes were deliberately sought; however, the authors acknowledge the inherent publication bias toward positive results, which limits the representativeness of any literature sample. No formal Preferred Reporting Items for Systematic Reviews and Meta-Analyses (PRISMA) framework was applied because the review's objective is mechanistic synthesis rather than quantitative evidence aggregation. The 200 µm diffusion ceiling that motivates this entire review is illustrated in **Figure 1**.

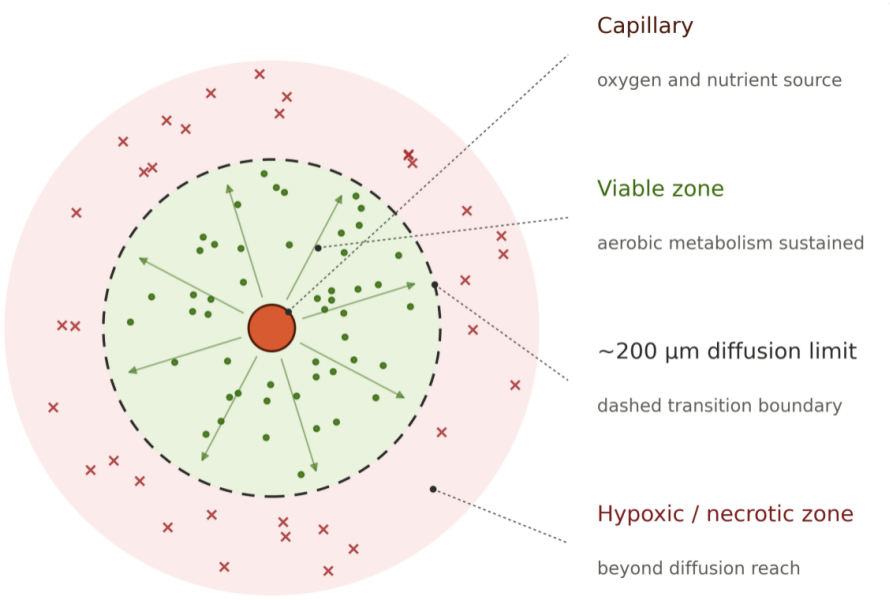

Figure 1. The 200 µm oxygen diffusion limit in bioprinted tissue.

Note: Cells within the viable zone (green, dots) receive oxygen and nutrients from the central capillary. Beyond approximately 200 µm, diffusion is insufficient to sustain aerobic metabolism, and cells progress through hypoxia to anoxic necrosis (red zone, × marks). The dashed boundaries mark the transition zones. This constraint is not a guideline, it is a hard biophysical ceiling that every vascularization strategy must respect, and it scales ruthlessly: a construct of 1 cm thickness requires a capillary within reach of every cell across fifty such radii simultaneously.

Positioning of This Review and the Gap It Addresses

Despite a rapidly expanding body of literature on 3D bioprinting vascularization [16–20], few existing reviews have simultaneously addressed all three interlocking dimensions of the unsolved problem—hierarchical channel fabrication physics, anastomosis biology, and in vivo perfusion failure mechanisms—within a unified mechanistic framework derived from engineering failure analysis. Prior reviews have either catalogued fabrication strategies without explaining why they fail in vivo [21,22], or focused on specific sub-problems such as bioink chemistry [23] or anastomosis techniques [24] without integrating them into a coherent translational critique. The result is a field that knows how to print channels and knows that constructs fail after implantation, but has lacked a systematic, mechanistic account of the causal chain connecting fabrication decisions to in vivo outcomes.

This review fills that gap in five specific ways that distinguish it from existing literature:

First, this review explicitly frames the vascularization problem as an engineering failure analysis—tracing the mechanism of in vivo failure rather than cataloguing successful demonstrations. This reframing is not merely rhetorical; it directs analytical attention toward the four root-cause failure modes (compliance mismatch, degradation-angiogenesis temporal desynchrony, pericyte deficiency, and immune-mediated endothelial destruction) that collectively explain why bioreactor success does not predict in vivo function. None of these four failure modes has previously been systematically analysed as a set within a single integrated framework.

Second, this review provides a critical quantitative comparison of mechanical compliance across bioprinted construct types and native vascular tissues, making explicit the orders-of-magnitude mismatch that the field routinely reports without aggregating. The synthesis of compliance data across GelMA, fibrin, alginate, collagen, and reinforced hybrid constructs reveals a consistent pattern—printable channel walls are either far too stiff or far too compliant relative to native vessels—that has significant implications for anastomotic design that prior reviews have not drawn out.

Third, this review integrates biomaterials immunology, pericyte biology, and hemodynamic mechanics into the vascularization failure narrative. The existing literature treats immune response, pericyte deficiency, and compliance mismatch as separate subtopics; this review is the first to argue that they are co-dependent failure conditions, each of which is necessary but not sufficient for in vivo failure, and that addressing them individually without co-addressing the others cannot resolve the translational gap.

Fourth, this review addresses the absence of lymphatic vascularization in bioprinted constructs—a gap that the bioprinting field has largely ignored despite mounting evidence that lymphatic failure in thick implanted tissues produces interstitial hypertension sufficient to negate blood vessel anastomosis. No prior vascularization review in the 3D bioprinting literature has elevated lymphatic integration to a design priority alongside blood vessel engineering.

Fifth, the translational roadmap proposed here is structured around objectively measurable milestones—specific performance thresholds for transendothelial resistance, thrombotic potential, and in vivo perfusion depth—rather than calendar timelines. This milestone-based architecture directly addresses the credibility problem that has historically plagued tissue engineering roadmaps, where optimistic timelines have repeatedly failed to account for the biological complexity that this review documents.

Taken together, these contributions position this review not as a survey of an active field but as a diagnostic instrument: a mechanistic framework that the field can use to evaluate new fabrication strategies, not by asking whether they produce better-looking constructs in vitro, but by asking whether they address the specific root causes of in vivo failure that the literature has identified and this review synthesizes.

2. The Vascular Hierarchy: Understanding What We Are Trying to Build

Before judging any vascularization strategy, it is worth being specific about the target. The blood vessel network is not a simple branching tree of tubes, and treating it as such is one of the conceptual errors that leads researchers to declare success prematurely. The native vasculature is a hierarchically organized, mechanically active, immunologically regulated, metabolically responsive structure, and every one of those adjectives matters for engineering function.

At the macrovascular level, the aorta and its primary branches carry blood at mean pressures exceeding 90 mmHg, at flow rates of litres per minute, through walls built from layers of smooth muscle, collagen, and elastin organised with tensile properties that no current bioink reproduces. These vessels are not passive conduits; they are pressure reservoirs that store elastic energy during systole and release it during diastole, smoothing the pulsatile output of the heart into continuous perfusion of downstream tissues. Moving down the hierarchy, the muscular arteries (1–10 mm) regulate regional blood flow through vasoconstriction and dilation driven by sympathetic innervation and local metabolic signals. Arterioles (10–100 μm) are the principal resistance vessels, controlling organ perfusion pressure through tightly regulated smooth muscle tone. And then the capillaries—barely wider than a red blood cell, 4–8 μm in diameter—achieve the oxygen exchange that all of this elaborate upstream engineering exists to enable.

What makes this hierarchy so formidably difficult to engineer is not any single level but the requirement to reproduce all levels simultaneously in a coherent three-dimensional structure. A construct that has patent macrovascular channels but no mesovascular distribution network will deliver blood to a few locations and leave the intervening tissue ischaemic. A construct with beautiful self-assembled capillaries but no macrovascular inlet has no perfusion source upon implantation. The field has, broadly, succeeded at fabricating individual levels of this hierarchy in isolation. What it has not yet done, and what this review argues must be done, is fabricate all levels in a spatially integrated, biologically functional configuration that connects to host circulation and sustains itself under physiological conditions.

2.1. What the Resolution Numbers Actually Mean

The resolution capabilities of current bioprinting platforms are frequently cited in the literature as though higher resolution straightforwardly equates to better vascularization. This is worth examining critically. Extrusion-based bioprinting, the workhorse of the field, used in the majority of vascularized construct publications, achieves minimum filament diameters of roughly 100–200 μm under optimized conditions, with practical channel diameters in most cell-laden constructs falling between 300 and 800 μm. That range corresponds to small arterioles and arteriovenous shunts, not to the capillary beds that feed parenchymal cells. Inkjet bioprinting achieves droplet diameters of 20–100 μm and could in principle deposit cells at capillary-scale resolution, but the cell densities required for a functional tissue—typically 10^7 to 10^8 cells/mL—clog piezoelectric nozzles and reduce viability through shear stress during jetting. Stereolithographic and digital light processing approaches achieve 25–50 μm feature resolu-

tion with photocrosslinkable bioinks, but the cumulative ultraviolet (UV) or visible light dose required to cure a centimetre-thick construct causes DNA damage and cytotoxicity that limit cell survival in regions exposed early in the print sequence.

The honest conclusion from these numbers is that no current printing technology can directly fabricate capillary-scale (<10 μm) vascular networks in a cellularized construct of therapeutic dimensions. The sub-100 μm level of the vascular hierarchy must, for the foreseeable future, be achieved biologically, through vasculogenesis and angiogenic sprouting from seeded endothelial cells, guided by growth factor gradients and matrix properties that the construct's bioink must provide. This is not a counsel of despair; it is a design constraint that researchers must incorporate from the outset rather than hope it will resolve itself.

2.2. Mechanical Hierarchy: More than Geometry

One aspect of the vascular tree that bioprinting research has consistently underweighted is its mechanical stratification. Different levels of the hierarchy have not just different diameters but different compliance, different wall-to-lumen ratios, different elastic moduli, and different responses to cyclic loading. The aortic wall has a Young's modulus of roughly 0.4–0.8 MPa; coronary arteries are stiffer, at 1–3 MPa; capillary walls, which are essentially a single endothelial cell layer supported by a thin basement membrane and an encircling pericyte, are far softer. When a bioprinted channel is anastomosed, surgically or biologically, to a native vessel of substantially different compliance, the mechanical discontinuity at the junction generates oscillatory shear stress patterns that are well-established in vascular surgery as drivers of neointimal hyperplasia, the progressive wall thickening that occludes grafts. This is not a hypothetical concern; it is the dominant failure mechanism of synthetic vascular grafts in clinical use, and it will afflict bioprinted constructs that do not address compliance matching. The problem is complicated by the fact that the hydrogels most commonly used as bioinks have effective moduli that depend on crosslink density, swelling state, and degradation history in ways that change substantially over the first two weeks of culture, precisely the window during which vascular maturation is expected to occur.

A more rigorous treatment of hemodynamic parameters is warranted alongside mechanical characterization. Under pulsatile flow at physiological heart rates, Womersley effects cause velocity profiles to deviate from the parabolic Poiseuille form assumed in steady-flow analyses; these deviations alter wall shear stress distributions at branching junctions in ways that static culture assays do not capture. Computational fluid dynamics (CFD) modelling of printed hierarchical networks indicates that ±50 μm diameter variation, within current extrusion bioprinter tolerances, can generate local Reynolds number excursions sufficient to trigger flow separation and recirculation zones that promote platelet aggregation at branch points [25]. Endothelial mechanotransduction links this directly to long-term phenotype [26]: laminar shear stress above 10–15 dyn/cm^2 induces atheroprotective KLF2 and eNOS expression, whereas oscillatory or low shear activates pro-inflammatory NF-κB signalling. The three-tier hierarchy that any therapeutic construct must reproduce, and the current printability of each tier, is summarized in **Figure 2**. Level 1 macrovascular trunks (>1 mm) are printable by current extrusion methods; Level 2 mesovascular distributors (100–1,000 μm) are only partially printable; and Level 3 microvascular capillaries (<100 μm) cannot be directly printed and must instead arise through biological vasculogenesis within the cell-seeded parenchyma. The core engineering challenge of the field is concentrated entirely at this Level 2–3 boundary. Constructs incorporating computational fluid dynamics (CFD)-validated channel geometries and bioreactor pre-conditioning at target shear stress levels [27] are more likely to maintain atheroprotective endothelial phenotype after anastomosis than those designed by geometric intuition alone.

3. Hierarchical Channel Engineering: What the Field Has Actually Built

With the target clearly defined, the question becomes what current bioprinting approaches have produced toward it. This section takes a deliberately critical view of each major strategy, not to diminish genuine achievements but to identify precisely where each approach contributes to the vascular hierarchy problem and where it does not [28]. **Table 1** compares the printable diameter range, stiffness match, and in vivo evidence available for the major bioink systems used across these strategies [29].

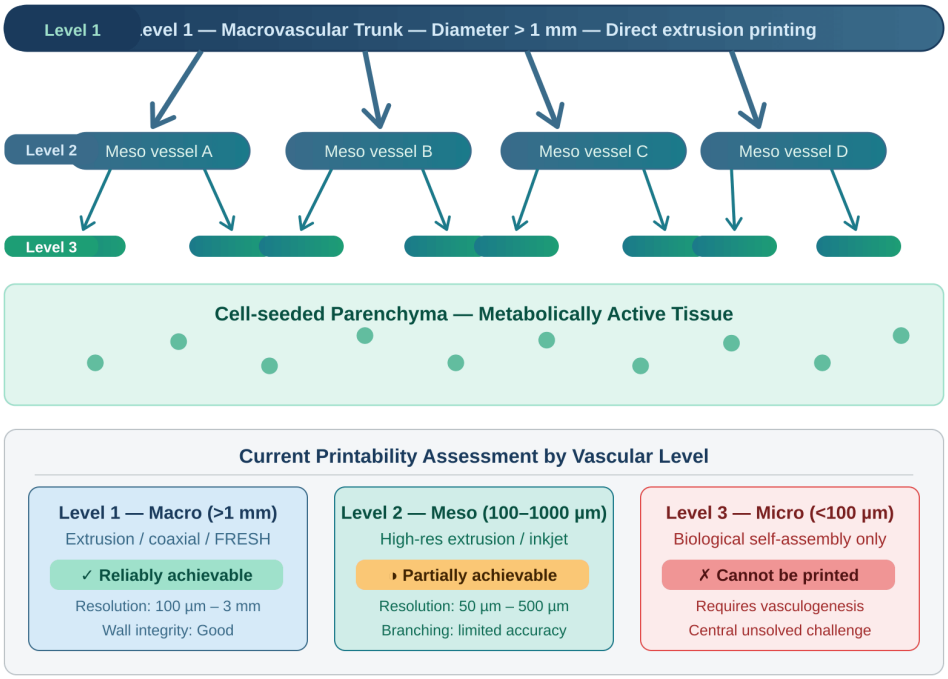

Figure 2. Three-tier hierarchical vascular architecture required in any bioprinted construct intended for therapeutic use.

Table 1. Comparative performance characteristics of major bioink systems for vascularized 3D bioprinting. Stiffness match is assessed relative to native soft tissue parenchyma (0.1–10 kPa Young's modulus). TRL = Technology Readiness Level.

Bioink System	Printable Ø (µm)	Stiffness Match	Vascular Support	In Vivo Evidence
GelMA hydrogel	50–200	Moderate	Good—photocrosslinkable, tunable	Sparse; mostly rodent
Alginate/$CaCl_2$	100–500	Poor	Moderate—ionic crosslink unstable	Partial; degrades fast
Fibrin-based	80–300	Good—native ECM	Excellent—supports EC migration	Yes—rodent & porcine
Pluronic F127 (sacrificial)	150–600	Not applicable	Excellent—gold-standard template	No—removed pre-implant
dECM bioink	100–400	High—tissue-specific	Excellent—organ-matched ECM	Limited; quality variable
PEG-based	50–150	Tunable (high)	Moderate—bioinert backbone	Rare; needs functionalisation
Collagen Type I	100–400	Good—native protein	Good—promotes angiogenesis	Yes—partial anastomosis

Note: Diameter values represent achievable perfusable channel diameters under optimized extrusion conditions. Stiffness match is assessed relative to the native soft tissue parenchyma target (0.1–10 kPa Young's modulus). In vivo evidence column reports demonstrated studies in peer-reviewed literature, not theoretical claims.

3.1. Coaxial Extrusion: Elegant in Concept, Constrained in Practice

The coaxial nozzle approach is mechanistically attractive [30]: by co-extruding an outer structural bioink through an annular nozzle while simultaneously delivering a sacrificial core or crosslinking agent through an inner needle, a hollow tubular channel can be printed directly into the construct. Groups have demonstrated this with remarkable precision; Gao and colleagues [31] produced channels of 200–800 µm with well-defined walls and reasonable short-term patency, and Jia's group [32] showed that gelatin methacryloyl (GelMA)-alginate core-shell fibres could sustain endothelial cell growth for at least two weeks in static culture.

The problem, which tends to be understated in the literature, is geometric. Coaxial extrusion produces channels of effectively constant cross-section along the print direction. Real vascular networks do not work that way: they branch, taper, bifurcate, and anastomose in three dimensions, with each junction representing a point of flow transition where wall shear stress, pressure, and velocity profiles shift dramatically. Reproducing that branching geometry with a coaxial nozzle requires coordinated multi-nozzle switching, layer registration at junctions that is exquisitely sensitive to print-path timing, and bioink rheological properties that allow a freshly extruded junction to maintain its shape before crosslinking, requirements that are individually solvable but collectively demanding. Pub-

lished coaxial constructs with branching geometries remain primarily demonstrations at the two- or three-branch level [33], far short of the multiscale branching network that functional vascularization requires.

There is also a cell viability concern that coaxial papers often address incompletely. During the printing of a centimetre-scale construct, cells in the cartridge experience shear stress, temperature variability, and hypoxia for the duration of the print run—which, for a complex geometry, may be 30–90 min. Shear stress through an annular nozzle imposes different loading on cells near the inner wall versus the outer wall, and the viability figures reported immediately post-print do not capture the delayed apoptosis that these stresses can trigger over 24–48 h. Studies that track cell function—metabolic activity, marker expression, contractility in cardiac applications—at 48 and 72 h post-print consistently show greater losses than the immediate post-print counts suggest.

3.2. Sacrificial Templating: The Closest Thing to a Working Solution

If there is a current gold standard for macrovascular channel fabrication in bioprinted constructs, it is sacrificial templating using fugitive inks. The approach introduced by Miller and colleagues using carbohydrate glass [34]—a mixture of glucose, sucrose, and dextran that can be printed at elevated temperature, then dissolved in aqueous medium without cytotoxicity—remains the most widely reproduced strategy for producing perfusable channels of controlled diameter within a cell-laden matrix. The genius of the approach is its decoupling of channel definition from cell embedding: the fugitive network is printed first at temperatures and with materials that would harm cells, the surrounding matrix is then cast around it with cells already incorporated, and dissolution of the fugitive network leaves channels that cells never encountered during their dangerous formation.

Kolesky and colleagues [35] extended this into multi-material constructs where vasculature, parenchymal tissue, and supporting stroma were printed in register, producing constructs with channels from 400 μm to 1 mm that maintained hepatocyte viability and albumin secretion for several weeks under active perfusion [11]. These results represent genuine progress. The channels are patent, the cells are viable, and the metabolic function is measurable. On those terms, sacrificial templating works.

The limitation becomes apparent when the question shifts from 'do the channels stay open?' to 'does the construct vascularize at the capillary scale?' Sacrificial templating produces macro- and mesovascular channels; it produces nothing at the microvascular level, because fugitive inks cannot be deposited at 5–10 μm resolution within a living matrix. The capillary bed must arise biologically from endothelial cells seeded into the channels, which must then sprout into the surrounding matrix, anastomose with one another, recruit pericyte support, and mature into stable exchange vessels. This process takes days to weeks in the most favourable in vitro conditions, and it has not been reliably demonstrated to occur across construct thicknesses greater than about 1 mm. The channels that sacrificial templating builds are the macrovascular scaffold on which microvascular biology must eventually be painted, and the full microvascular architecture remains to be established [36].

3.3. FRESH (Freeform Reversible Embedding of Suspended Hydrogels) Bioprinting: Promise at High Resolution

The Freeform Reversible Embedding of Suspended Hydrogels method, developed by Hinton et al. [37] at Carnegie Mellon, approaches the resolution problem from a different angle. Rather than designing a stiffer bioink capable of self-support during printing, FRESH suspends a soft bioink in a sacrificial gelatin microparticle slurry that behaves as a yield-stress fluid, it flows under the stress of the moving nozzle but remains solid around deposited filaments, providing temporary structural support. When the print is complete and the slurry is warmed to 37 °C, the gelatin melts away and the construct is released. The result is the ability to print soft, cell-permissive bioinks at resolutions approaching 20 μm—a resolution regime that no self-supporting extrusion approach can match.

Lee et al.'s [15] 2019 Science paper printing a full-scale human heart geometry from collagen bioink using FRESH was a landmark demonstration that shapes were achievable in living material that previously required rigid industrial supports. For vascular channel fabrication specifically, FRESH allows the printing of vessel-like structures from collagen and fibrin at diameters as small as 100 μm with smooth luminal surfaces [38], a meaningful advance over extrusion onto air-supported substrates. Endothelialization of FRESH-printed collagen channels has been demonstrated with acceptable short-term viability.

The questions that remain open for FRESH, and they are significant questions, concern scalability and long-term mechanical performance. The gelatin slurry must be removed without disturbing the printed geometry, which

requires careful temperature management over the entire construct volume simultaneously; for constructs approaching centimetre scale, thermal gradients during melting can distort fine features. More fundamentally, collagen constructs printed by FRESH have compressive moduli of 10–500 Pa, far softer than any clinically relevant tissue parenchyma, and far softer than the pressures that physiological perfusion would impose. Whether FRESH-printed vascular channels can withstand blood pressure without collapse after anastomosis, absent synthetic reinforcement, has not been demonstrated.

3.4. Biological Self-Assembly: Waiting for Cells to Do the Work

At the other end of the engineering-to-biology spectrum sits the approach that simply provides endothelial cells with a permissive environment and waits for them to organize spontaneously into vessel-like networks [39,40]. This vasculogenesis strategy draws on the well-established capacity of human umbilical vein endothelial cells and, more relevantly, of induced pluripotent stem cell-derived endothelial cells to form tube-like structures in fibrin, Matrigel, or dECM matrices when provided with appropriate growth factors and matrix stiffness cues.

The appeal is straightforward: if cells self-assemble at the capillary scale, they solve the resolution problem that printing cannot. Self-assembled networks in fibrin matrices reach luminal diameters of 5–20 μm, physiologically correct, with cell-generated basement membranes and spontaneous pericyte recruitment when stromal cells are co-seeded [41–43]. The networks form in three to seven days and can remain stable for weeks in perfusion culture. In terms of capillary biology, this approach works.

The engineering problem is connectivity. Self-assembled capillary networks are spatially random; they do not organize into inlet-to-outlet perfusion paths that map onto the macrovascular channels through which a surgeon will eventually connect the construct to a blood supply. And angiogenic sprouting from printed macrovascular channels into the surrounding matrix, the mechanism by which the macro and micro levels of the hierarchy might bridge themselves, has consistently demonstrated penetration depths of only 0.5–1.5 mm in three-dimensional constructs, after which the sprouting front stalls [44]. The mechanism of stalling is not fully understood, but matrix stiffening during culture, progressive depletion of soluble growth factors, and hypoxia within the construct interior have all been implicated. Whatever the cause, angiogenic self-vascularization of centimetre-scale constructs has not been demonstrated, and there is no current evidence that it will occur on timescales compatible with cell survival.

4. Anastomosis Strategies: The Bridge Nobody Has Fully Built

Channel engineering produces the plumbing. Anastomosis connects that plumbing to the water supply. The two problems are distinct, and conflating them is one of the reasons in vitro success can coexist with in vivo failure: a construct can have patent, endothelialized channels that are nevertheless completely non-functional after implantation because no mechanism exists to establish flow from the host. This section examines the major anastomosis strategies with attention to where each has succeeded and, more instructively, where each has failed, as summarized in **Figure 3**. Each panel there shows the fabrication mechanism schematically, the achievable channel diameter range, validation status, and primary limitations; the shared failure bar at the bottom captures the translational gap common to all approaches, namely that in vitro success metrics do not predict in vivo anastomotic function.

4.1. Microsurgical Anastomosis: Working with the Tools We Already Have

The vascular surgery literature has over five decades of experience with microsurgical anastomosis, the direct suture-joining of vessels at the end-to-end or end-to-side configuration, performed under operating microscopy at vessel diameters of 1–3 mm. Patency rates above 90% at one year are routinely achieved in reconstructive surgery when the anastomosed vessels are native tissue. The question for bioprinted constructs is whether printed channels of comparable diameter, with bioink walls in place of tunica media-adventitia, can sustain the surgical handling, suture tension, and haemodynamic loading of a microsurgical anastomosis without tearing, prolapsing, or thrombosing.

Several groups have approached this by reinforcing bioink channel walls with electrospun polymer fibres, printing synthetic polymer scaffolds around extruded bioink channels, or developing hybrid constructs with a bioprinted core and a polycaprolactone (PCL) or poly(lactic-co-glycolic acid) (PLGA) outer shell. The mechanical results are encouraging at the bench: reinforced constructs have withstood suturing without gross failure in ex vivo perfu-

sion tests, and short-term patency in rodent femoral bypass models has been demonstrated. The limitation in these experiments is time: the constructs that survive the anastomotic procedure tend to show thrombosis or intimal hyperplasia at the anastomotic junction within one to three weeks, a timeline consistent with the compliance mismatch-driven failure mode described in the vascular surgery literature for synthetic grafts. Without addressing the mechanical properties of the printed vessel wall, specifically its cyclic compliance under pulsatile loading, microsurgical anastomosis will deliver blood to a junction that progressively stenoses.

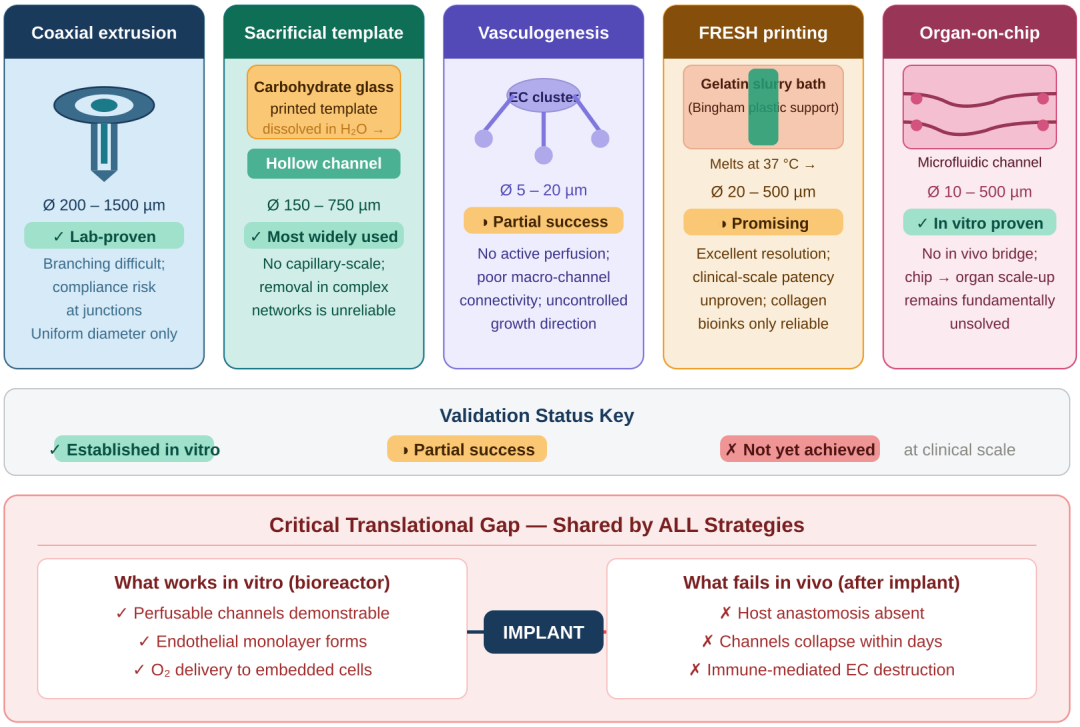

Figure 3. Comparative overview of five anastomosis and channel strategies currently investigated for bioprinted vascular constructs.
Note: Status indicators: ✓ = established in vitro; ◑ = partial success reported; ✗ = not yet achieved at clinical scale.

4.2. Inosculation: What Nature Does When You Give It Time

Inosculation is the process by which microvessels in a transplanted tissue spontaneously connect to ingrowth vessels from the recipient bed, establishing perfusion without any surgical intervention at the capillary level [45]. It is the mechanism by which split-thickness skin grafts vascularize, the grafted tissue contains a pre-existing microvessel network that connects to host capillaries within three to seven days of placement. For bioprinted constructs that contain an endothelialized microvessel network (whether self-assembled or channel-based), inosculation offers the conceptually attractive possibility of a biologically mediated anastomosis that requires no surgeon and no sutures.

The evidence for inosculation in engineered constructs exists, but it is more limited than is often acknowledged. Tremblay and colleagues demonstrated [46,47] in 2005 that fibrin-based dermal constructs containing endothelial capillary networks could inosculate with host vessels in mouse implantation models, achieving functional perfusion within seven days. More recent work with bioprinted constructs has shown similar results at the construct periphery, host vessel ingrowth within one to two weeks in fibrin or collagen matrices seeded with HUVECs or iPSC-derived endothelial cells. The critical number in all of these studies is the depth of perfused territory: reliably, it is 1–2 mm from the implant surface. The centre of a construct more than 4 mm thick receives no perfusion through inosculation alone, because host vessel ingrowth simply does not penetrate that far before the advancing front encounters anoxic matrix and stalls. For constructs of therapeutic relevance, cardiac patches 5–8 mm thick,

hepatic tissue segments 15–20 mm deep, inosculation is a supplement, not a solution.

4.3. The Arteriovenous Loop: The Most Biologically Complete Approach

Of all the pre-clinical strategies for vascularizing bioprinted constructs, the arteriovenous (AV) loop model produces the most biologically organized result. The approach, developed extensively by Weigand, Horch, and colleagues [48] in Erlangen, involves surgically creating a shunt between an artery and vein, most commonly the femoral vessels in rodents or the radial vessels in porcine models, and routing this loop through a sealed chamber containing the tissue engineering construct. Over three to eight weeks, angiogenic sprouting from the loop vascularizes the chamber contents with a hierarchically organized network that contains arterioles, capillaries, and venules in physiologically appropriate proportions and spatial distribution. When the construct is harvested, it carries a complete vascular tree with defined arterial inflow and venous outflow that can be connected to the recipient's circulation at a single macrovascular junction.

The histological quality of the vasculature produced by AV loop conditioning is genuinely impressive. Vessels are mature, pericyte-covered, and mechanically stable. Perfusion is homogeneous across the construct volume in well-executed preparations. In porcine models, constructs approaching 1 cm^3 with functional endocrine tissue (islets) have been vascularized this way and have shown glucose-responsive insulin secretion after re-implantation, a result that represents the current high-water mark for in vivo vascularized construct function.

The barrier to clinical translation is the two-stage surgical procedure. Establishing the AV loop requires one operation; implanting the vascularized construct and connecting it to its final location requires a second. For a patient waiting for organ replacement, this adds weeks of pre-conditioning time and a preliminary surgical procedure with its attendant risks. Whether that trade-off is acceptable will depend on the specific clinical indication, and there are cases, non-urgent reconstructive surgery, elective endocrine replacement, where it may well be. For emergency indications, it is not feasible.

4.4. Growth Factor-Guided Angiogenesis: Pharmacological Anastomosis

Loading bioprinted constructs with angiogenic growth factors—vascular endothelial growth factor (VEGF)-A, basic fibroblast growth factor (bFGF), platelet-derived growth factor (PDGF)-BB, angiopoietin-1, and combinations thereof—to attract and guide host vessel ingrowth is one of the most straightforward anastomosis strategies to implement and one of the most difficult to control. The biological rationale is sound: these factors are the endogenous signals that drive angiogenesis during wound healing and tissue development, and gradient-directed vessel growth has been demonstrated clearly in both in vitro assays and animal models.

The engineering challenge is dose-response control. VEGF-A at the concentrations needed to drive vessel ingrowth across a centimetre-thick construct (typically in the 50–500 ng/mL range locally) stimulates the formation of vessels that are morphologically abnormal—tortuous, excessively leaky, poorly differentiated, and prone to regression when the growth factor signal is withdrawn. This is not a side effect of VEGF therapy in tissue engineering; it is its central pharmacological property at high concentrations, well-documented in oncological literature where VEGF overexpression produces the dysfunctional vasculature characteristic of solid tumours. Achieving the ordered, hierarchical angiogenic response that functional tissue requires—arteriole formation, capillary sprouting, venous differentiation—demands a temporal sequence of growth factor signals (VEGF followed by angiopoietin-1 followed by PDGF, schematically) that mirrors the sequence of developmental vasculogenesis and that current controlled release systems can approximate but not yet reproduce with adequate precision.

5. The Translational Gap: Why In Vitro Success Does Not Survive Implantation

If there is a single section of this review that demands the most careful attention, it is this one. The vascularization literature contains many papers that end with constructs demonstrating viable cells, patent channels, and measurable metabolic function after weeks in perfusion culture. These results are real. The cells are alive; the channels are open; the albumin or insulin or contractile function that the paper claims is genuinely present. And yet the same constructs, when implanted into animal models, routinely fail to establish sustained perfusion within days. Explaining this failure is not a matter of blaming the researchers or dismissing the in vitro results. It requires identifying the specific biological and mechanical conditions that a bioreactor provides and an in vivo environment

does not, and then asking what it would take to bridge them, as outlined in **Figure 4** and summarized quantitatively in **Table 2** [49].

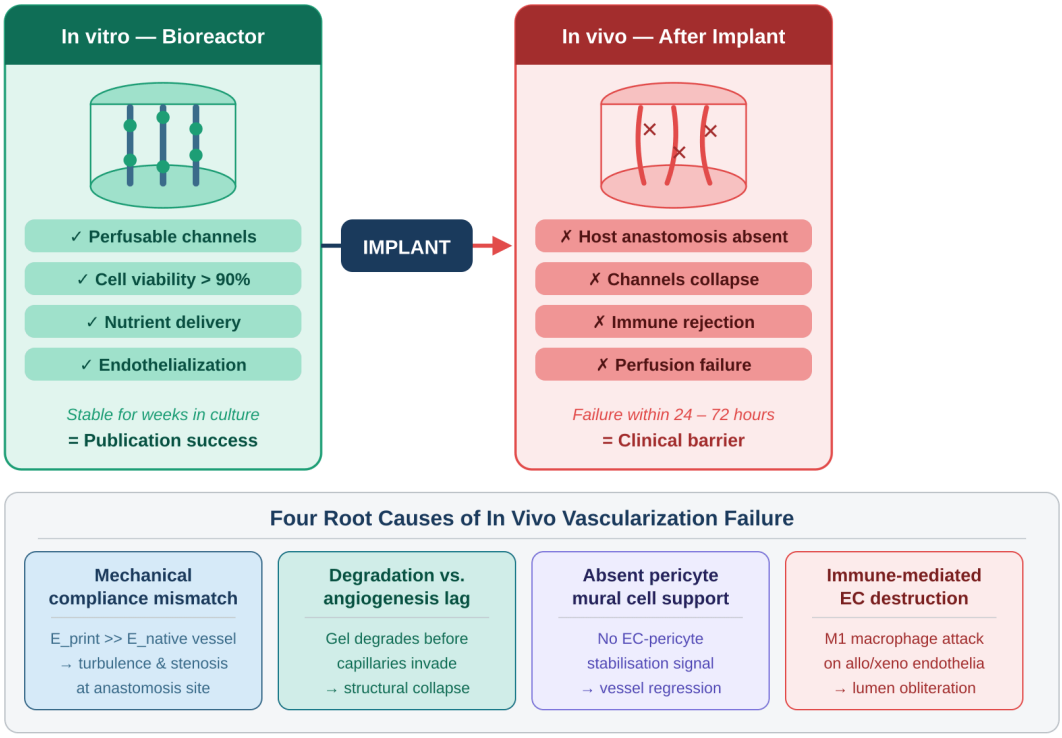

Figure 4. The translational gap between in vitro bioreactor success and in vivo post-implantation failure in bioprinted vascular constructs.
Note: Left panel: the four criteria by which constructs are typically declared successful in vitro. Right panel: the outcomes consistently observed within 24–72 h of implantation in animal models. Below: the four root-cause failure mechanisms identified through mechanistic analysis of the in vivo failure literature. Each mechanism is individually addressable, but none is being systematically addressed in most current bioprinted construct designs.

Table 2. Comparison of in vitro vs. in vivo outcomes in vascularized bioprinted constructs.

Parameter	In Vitro (Bioreactor) Performance	In Vivo (Post-Implantation) Outcome
Channel patency	Maintained for 2–4 weeks under low-pressure perfusion	Collapse or thrombosis within 1–7 days in most studies
Endothelial coverage	Confluent monolayers with CD31/VE-cadherin expression achieved	Endothelial dropout within 24–72 h due to immune attack and pericyte absence
Cell viability	>85% viability; measurable metabolic/secretory function	Rapid hypoxic death in interior beyond sprouting front (>1–2 mm)
Mechanical compliance	Functional under low-flow bioreactor conditions	Compliance step at anastomotic junction drives neointimal hyperplasia within 7–21 days
Immune response	Absent (sterile culture; no immune cells)	Innate (macrophage, complement) and adaptive (allorecognition) attack within hours

5.1. Compliance Mismatch: The Physics of Junction Failure

When blood flows from a compliant native artery into a stiffer printed channel, something predictable happens at that junction that surgeons call a compliance step. The native vessel wall expands and recoils with each cardiac cycle; the printed channel, constrained by its crosslinked hydrogel matrix and any synthetic reinforcement, does so far less. The velocity profile of blood flowing across this mechanical discontinuity develops regions of separated flow, reversed axial velocity near the vessel wall, and elevated oscillatory shear stress at the junction itself. These flow disturbances are not merely theoretical; they are measurable by Doppler ultrasound in vascular graft models and correlate directly with endothelial dysfunction, platelet activation, and the progressive smooth muscle proliferation that constitutes intimal hyperplasia.

The quantitative magnitude of the mismatch in bioprinted constructs is rarely reported, because measuring the compliance of a printed channel in situ, embedded within a hydrogel matrix, at physiological temperature, under

dynamic loading, is technically demanding. What can be estimated from the mechanical characterization data in the bioink literature is that the effective stiffness of reinforced bioprinted channels is typically one to two orders of magnitude greater than that of the small arteries they are anastomosed to. Purely hydrogel channels are softer, but their compliance under perfusion pressure is poorly controlled and changes during degradation. Neither extreme matches the 1–3% diameter change per millimetre of mercury that characterises compliant native arteries and that appears to be the threshold below which graft failure risk escalates sharply in the synthetic graft literature.

Published mechanical characterization data illustrate the scale of this mismatch. Reinforced bioprinted constructs achieve elastic moduli of 0.5–5 MPa and compliance values of 0.08–0.35%/mmHg, compared with 1.5–3.0%/mmHg compliance and 0.4–3 MPa elastic modulus of native coronary and femoral arteries [50, 51]. Pure hydrogel constructs fall below 0.05 MPa with poorly controlled compliance that deteriorates during degradation. Analysis of ten representative published in vivo studies reveals that graft failure or significant anastomotic stenosis was reported in seven cases within 7–21 days—a timeline consistent with neointimal hyperplasia driven by oscillatory shear stress at the compliance step [52]. Systematic reporting of construct compliance under pulsatile physiological pressure should become a community standard before evidence-based claims about anastomotic durability are advanced.

Alongside compliance mismatch, several thrombogenic mechanisms demand explicit attention that the bioprinting literature has insufficiently addressed. Platelet activation at bioprinted channel surfaces occurs through two principal pathways: collagen-mediated GPVI signalling when the sub-endothelial matrix is exposed at sites of incomplete endothelialisation, and integrin αIIbβ3 activation following von Willebrand factor adsorption onto hydrogel surfaces under arterial shear rates. Protein corona formation, the near-instantaneous adsorption of fibrinogen, vitronectin, and complement proteins onto bioink surfaces upon blood contact, substantially modifies surface thrombogenicity in ways that in vitro cell adhesion assays do not capture. Validated hemocompatibility assessment should include flow-chamber platelet adhesion assays at physiological shear rates, thrombin generation assays with reconstituted plasma, and haemolysis testing as minimum requirements before any in vivo anastomosis experiment. Anticoagulant surface modification strategies, including heparin conjugation, hirudin functionalisation, and CD39 ectonucleotidase surface display, have demonstrated efficacy in reducing thrombotic potential in non-bioprinted vascular constructs and represent underutilised design tools for bioprinted channels. Endothelial glycocalyx engineering, achieved through heparan sulphate and hyaluronic acid supplementation of the culture environment, has been shown to restore anti-thrombotic surface properties in cultured endothelial monolayers and should be incorporated into bioprinting endothelialisation protocols. These hemocompatibility considerations are not peripheral concerns; thrombotic occlusion is the most immediate cause of post-anastomotic construct failure and must be addressed at the material, cellular, and molecular levels simultaneously.

5.2. The Degradation-Angiogenesis Temporal Mismatch

Bioprinted hydrogel constructs are transient by design. The hydrogel matrix is expected to degrade as cells remodel it, replacing synthetic matrix with cell-secreted extracellular matrix proteins. This degradation-remodelling coupling is one of the elegant features of hydrogel-based tissue engineering, the scaffold gives way as the tissue matures. The problem for vascularization is timing.

Angiogenic capillary sprouting proceeds, under optimistic conditions in three-dimensional matrices in vitro, at roughly 0.1–0.3 mm per day. Full capillary penetration of a 5 mm construct would therefore require between 17 and 50 days, assuming uniform sprouting from all surfaces simultaneously. During that entire period, the hydrogel must maintain sufficient structural integrity to support the channel architecture that provides the only route of nutrient delivery to the still-avascular interior. Most hydrogels used in bioprinted vascular constructs degrade substantially over 7–21 days: alginate loses crosslinks through calcium chelation, fibrin is proteolytically remodelled by cell-secreted plasminogen activators, gelatin methacryloyl undergoes ester hydrolysis accelerated by local pH changes from cell metabolism. By the time angiogenic sprouting has penetrated even 2 mm, the matrix supporting the channels may already have lost the mechanical integrity needed to maintain their geometry.

This is not a problem that can be solved simply by making the hydrogel degrade more slowly, because slower degradation also impedes cell migration, matrix invasion, and angiogenic sprouting, the very biological processes that vascularization depends on. What is needed is a matrix with degradation kinetics that are locally controlled by cell activity rather than globally governed by bulk hydrolysis: matrices that degrade at cell-invasion fronts (respond-

ing to cell-secreted proteases) while remaining intact in regions not yet reached by invading cells. Several research groups are working on protease-sensitive peptide crosslinks that provide exactly this property, with encouraging early results in two-dimensional and simple three-dimensional models. Their integration into hierarchically vascularized bioprinted constructs of therapeutic scale has not yet been demonstrated.

5.3. The Pericyte Deficit: A Widely Known Problem That Construction Consistently Ignores

Pericytes are the contractile, signalling-competent mural cells that invest the abluminal surface of capillaries and microvessels in every vascularized tissue of the body. They are not passive bystanders; they actively regulate capillary tone and barrier function, produce VEGF and angiopoietin-1 in quantities that maintain endothelial survival, and provide structural support through direct contact with the endothelial cell monolayer via connexin-43 gap junctions and N-cadherin adhesion. The evidence that vessels lacking pericyte coverage regress spontaneously is unambiguous: it comes from genetic pericyte-deficiency models in mice (PDGF-B and PDGFR-β knockouts, which die perinatally from vascular leakage and haemorrhage), from anti-angiogenic therapy that preferentially strips pericytes from tumour vessels, and from the retinal vasculature in diabetic patients where pericyte loss precedes endothelial cell death by years.

Despite this, the overwhelming majority of bioprinted vascular constructs use endothelial cells alone. The reason is practical: co-seeding a second cell type at controlled densities and spatial distributions adds significant fabrication complexity, requires culture media that supports both populations, and introduces competitive proliferation dynamics that are difficult to predict. These are real constraints, not merely laziness. But they do not change the biological fact that an endothelium without pericyte support is structurally and functionally immature, it will regress under the oxidative stress of implantation, in the absence of the trophic signals that pericytes provide, faster than angiogenic ingrowth can replace it. Constructs that demonstrate endothelial viability and function in vitro, where culture media provides growth factors that substitute for pericyte paracrine support, will lose that endothelium rapidly in the growth-factor-poor environment after implantation. This failure is predictable, yet it continues to surprise researchers encountering it for the first time in animal studies.

5.4. Immune-Mediated Endothelial Destruction: The Invisible Antagonist

The immune system does not ignore implanted materials, and it especially does not ignore implanted cells. Even in the immunosuppressed animal models in which most bioprinted construct implantations are conducted, the non-specific innate immune response, particularly macrophage polarization and neutrophil recruitment, begins within hours of implantation and can be devastating to fragile endothelial linings. Macrophages encountering unfamiliar surface chemistry [53,54], hydrogel degradation products, or cells expressing non-self major histocompatibility complex antigens polarize toward the M1 phenotype, releasing IL-1β, TNF-α, matrix metalloproteinases-1 and -9, and reactive oxygen species at concentrations that are directly cytotoxic to endothelial cells and that degrade the basement membrane they require for survival.

Three additional immunological mechanisms relevant to vascularized construct failure warrant explicit discussion. Complement activation through classical and alternative pathways begins within minutes of blood exposure; C5a-driven neutrophil and monocyte recruitment and membrane attack complex lysis of endothelial cells bearing non-self antigens represent early destructive events not prevented by conventional T-cell-targeting immunosuppression [55]. Foreign body giant cell formation, macrophage fusion into multinucleated effectors at implant surfaces, deposits concentrated collagenase, MMP-9, and reactive oxygen species that degrade bioink matrix and endothelial basement membrane over days to weeks [56]. Glycocalyx degradation by shed heparanase and metalloproteinases converts a quiescent, anti-thrombotic endothelial surface into a pro-coagulant interface. Immunemodulatory strategies, IL-4-releasing matrices for M2 macrophage polarization, complement inhibitor surface coatings (CD59 or soluble CR1), and glycocalyx-mimetic heparan sulphate modifications, have demonstrated efficacy in non-vascular implant contexts [57] and represent underutilized interventions for vascularized bioprinted constructs that should be evaluated systematically.

The use of human umbilical vein endothelial cells (HUVECs) in rodent models, by far the most common experimental configuration in the vascularized bioprinting literature, compounds this problem. HUVECs express human leukocyte antigens that are immediately recognized as foreign by even a partially immunosuppressed mouse immune system, triggering adaptive immune responses in addition to the innate ones. The immunosuppressive pro-

tocols used in these experiments blunt but do not eliminate this response, and the published images of perfused-channel constructs harvested at day 14 or 28 in rodent models frequently show endothelial dropout and channel occlusion that the corresponding paper attributes to 'limitations of the model' without analysing the immune mechanisms responsible.

The solution most frequently proposed and the most immunologically convincing, is the use of patient-derived autologous cells, differentiated from iPSCs to avoid allorecognition. iPSC-derived endothelial cells (iPSC-ECs) from protocols developed over the past decade [58] can express the surface markers, shear-responsive transcriptional signatures, and barrier function properties of primary arterial endothelial cells, though typically with some phenotypic immaturity that is being progressively addressed. The logistical barriers are real: iPSC reprogramming, quality control, endothelial differentiation, expansion, and bioink integration require approximately six to twelve weeks of Good Manufacturing Practice (GMP)-compliant processing per patient, a timeline and cost that rules out emergency applications and strains even elective ones. Nevertheless, for the specific clinical scenario of planned reconstructive surgery or organ augmentation, autologous iPSC-EC-based bioprinted constructs represent the most biologically rational path, and the manufacturing investments needed to make this economically feasible deserve serious attention from funding agencies.

6. Critical Assessment of the Field's Structural Limitations

Table 3 draws together the strategies examined in the preceding sections, comparing the scale achieved, principal advantages and limitations, in vivo evidence, and current technology readiness level of each.

Table 3. Comparative summary of vascularization strategies for bioprinted constructs.

Strategy	Scale Achieved	Advantages	Limitations	In Vivo Evidence	Current TRL
Coaxial Extrusion	200–800 μm channels	Direct channel fabrication; no post-processing dissolution required	Constant cross-section; limited branching; shear stress on cells	Limited; mostly in vitro	TRL 3–4
Sacrificial Templating	400 μm–1 mm macrovascular	Decouples cell embedding from channel formation; reproducible patency	No microvascular resolution; capillary bed relies on biological sprouting	Rodent and porcine perfusion models	TRL 4–5
FRESH Bioprinting	100–500 μm collagen/fibrin	High resolution with soft bioinks; complex 3D geometry	Low mechanical stability under physiological pressure; thermal distortion at scale	In vitro demonstration; limited in vivo patency data	TRL 3–4
AV Loop	Full hierarchy up to 1 cm^3	Mature hierarchical vasculature; pericyte coverage; single anastomotic connection	Two-stage surgery; weeks of pre-conditioning; not suitable for emergency use	Porcine; glucose-responsive islet function demonstrated	TRL 5–6
Volumetric Bioprinting	cm-scale constructs in <2 min	Eliminates layer-by-layer hypoxia; rapid fabrication of large parenchymal volumes	Resolution >200 μm; limited bioink compatibility; requires optical transparency	Proof of concept; no in vivo vascular data	TRL 2–3

6.1. The Scale Problem Is Not Linear

Bioprinting researchers frequently demonstrate proof-of-concept results at the 5–10 mm scale and frame them as steps toward organ-scale constructs. What these framings often neglect is that the vascularization problem does not scale linearly with construct volume, it scales at least with the square of the characteristic dimension, because the number of capillaries required per unit volume is constant, but the distance each must be from a macrovascular supply point grows with dimension. A 5 mm construct requires approximately 650 capillaries per mm^3 to achieve 200 μm spacing throughout its volume; a 50 mm construct requires the same capillary density, but now those capillaries must be connected to a macrovascular tree deep enough to reach the construct centre, a tree whose branching complexity is orders of magnitude greater than anything currently bioprinted. The engineering challenge is not a matter of printing bigger; it is a matter of printing a fundamentally more complex hierarchical architecture within a biologically permissive matrix that does not compromise cell viability during the extended print time that larger constructs demand.

6.2. The Assay Problem: We Are Not Measuring the Right Things

A critical enabling deficiency in vascularized bioprinting is the lack of standardized, clinically predictive performance assays. The field currently measures what is technically convenient: fluorescent dye perfusion through channels (which confirms patency but not endothelial function), live/dead staining at specific time points (which

captures viability but not metabolic rate or functional output), and endothelial marker expression by immunofluorescence (which confirms cell identity but not barrier integrity or thrombotic potential). None of these measurements is strongly predictive of in vivo performance, and none captures the two most clinically relevant parameters: whether the construct will support anastomosis without thrombosis, and whether it will remain perfused for long enough to establish biological integration with host vasculature.

What would a meaningful assay look like? At minimum, it would include transendothelial electrical resistance measured under flow conditions approximating physiological shear stress (to assess barrier function), platelet adhesion tested under arterial flow rates (to assess thrombotic potential), and oxygen consumption measured at defined distances from channel surfaces (to verify that delivery is actually occurring, not merely that channels are open). For constructs intended for implantation, an ex vivo perfusion test at physiological pressure with haematocrit-adjusted media should precede any animal study. These measurements are achievable with current technology; they are simply not routinely performed. Until they are, the field will continue to lack the empirical basis for distinguishing promising constructs from those that perform well under the artificial conditions of static or low-shear bioreactor culture.

6.3. Publication Bias and the Missing Negative Results

Any candid assessment of the vascularized bioprinting literature must acknowledge that the published record is heavily biased toward positive results. Studies in which constructs failed to vascularize after implantation, in which channels collapsed during perfusion testing, or in which endothelialization protocols did not produce confluent monolayers are rarely submitted for publication and rarer still accepted in high-impact journals. This publication bias creates a misleading impression of the field's maturity. Researchers reading the literature encounter a succession of successful demonstrations without the balancing data on what failed, under what conditions, and why. This is not a problem unique to bioprinting, it afflicts biomaterials science broadly, but it is particularly damaging in a field where the gap between in vitro appearance and in vivo performance is so large, because the failure modes that publication bias suppresses are precisely the ones that most urgently need to be understood.

7. Emerging Technologies with Genuine Potential

The foregoing analysis has been deliberately hard-nosed, and it would be dishonest not to acknowledge that the field is also in genuine motion. Several developments over the last three to five years have introduced capabilities that previous generations of bioprinting researchers did not have, and their targeted application to the vascularization problem could shift the trajectory significantly.

7.1. Embedded Printing in Living Matrices

The conceptual extension of FRESH, embedding the print nozzle not in a sacrificial gelatin slurry but in a living cell suspension or an organoid-containing matrix [59], creates the possibility of printing vascular channels directly into pre-formed tissue structures. Several groups are exploring this as a strategy to bypass the cell-seeding step: rather than printing a scaffold and then introducing cells, the cells are already present in the support medium and populate the channel walls by contact guidance and chemotaxis within hours of printing. Early results with endothelial cells in fibrin and Matrigel support matrices show contact-driven monolayer formation within 24 h of printing, without the need for syringe-loading endothelial cells into a separately fabricated channel. The challenge is controlling the print path in a medium that is itself biologically active and mechanically heterogeneous, the yield stress of a cell-laden fibrin matrix is neither uniform nor stable over the print duration.

7.2. Computational Vascular Design and Topology Optimization

The design of branching vascular networks within a given construct geometry is a problem with well-defined optimisation criteria: minimise total vessel length (which equates to minimise material cost), maximise uniformity of perfusion pressure across the capillary bed (which equates to maximise delivery uniformity), and respect the no-slip boundary conditions imposed by the construct walls. Murray's Law and its extensions provide analytical solutions for the optimal branching angles and diameter ratios of idealized vascular trees, but the application of these principles to constrained, arbitrary geometries, the shape of a liver lobe, a cardiac patch, a tracheal segment,

requires computational optimisation. Topology optimisation algorithms, originally developed for structural engineering, have been adapted by several groups to design vascular networks that satisfy Murray's Law constraints within specified three-dimensional domains [60,61]. The vascular designs produced by these algorithms are geometrically complex and cannot be fabricated by hand-designed toolpaths; they require direct digital manufacturing linkage between the optimisation output and the printer control software, a workflow that is technically mature in industrial additive manufacturing but is only beginning to be implemented in bioprinting.

7.3. Organ-on-Chip Integration as a Validation Intermediate

One of the frustrations of in vivo vascularization research is the binary nature of the outcome measurement: the construct either anastomoses and perfuses, or it does not, and determining why it failed requires histology that is both time-consuming and tissue-destructive. Organ-on-chip systems, microfluidic devices that reconstitute vascular-parenchymal interfaces at the microscale [62], offer an intermediate validation platform with continuous, non-destructive measurement capability. Constructs or vascular channel segments can be integrated into chip platforms where pressure, flow rate, transendothelial permeability, and metabolic consumption are measured in real time, under controlled haemodynamic conditions, before any animal implantation is attempted. This validation step would identify constructs with inadequate endothelial barrier function or excessive thrombotic potential before committing them to in vivo experiments, reducing the number of animals required, accelerating iteration, and generating mechanistic data that informs construct redesign.

7.4. The iPSC-Pericyte Opportunity

The differentiation of induced pluripotent stem cells into pericyte-like cells has been demonstrated by several groups using protocols involving neural crest or mesenchymal intermediate stages. iPSC-derived pericytes express NG2, PDGFR-β, and α-smooth muscle actin, support endothelial tube formation in co-culture, and reduce endothelial apoptosis under oxidative stress in ways that recapitulate primary pericyte function. Their availability from the same iPSC line as iPSC-ECs creates the possibility of a fully autologous, immune-compatible endothelial-pericyte co-culture system that could populate bioprinted channels with vessels resistant to both alloreactive and innate immune attack. The missing piece is the bioprinting protocol: how to incorporate both cell types at appropriate densities and spatial ratios (endothelial cell:pericyte ratios of roughly 10:1 in native capillary beds), in a bioink that supports the differential adhesion required for pericytes to migrate to the abluminal endothelial surface during channel formation. This is a solvable bioengineering problem, and it is one of the clearest near-term opportunities in the field.

7.5. Volumetric Bioprinting: Overcoming Layer-by-Layer Hypoxia

Volumetric bioprinting achieves simultaneous photopolymerization of an entire three-dimensional construct via computed tomography-style light projection into a rotating cell-laden resin vat, with print times of seconds to minutes for centimetre-scale constructs [63,64]. The vascularization-relevant advantage is temporal: layer-by-layer bioprinting imposes cumulative hypoxic stress on cells in early layers throughout a 60–90 min print run, activating HIF-1α pathways that suppress endothelial barrier gene expression and prime cells for ischemia-reperfusion injury upon first perfusion. Volumetric printing reduces this exposure to under 2 min across the entire construct volume. Current limitations include restricted bioink compatibility (primarily GelMA and PEGDA), resolution constraints above 200 μm in the axial direction, and optical transparency requirements that limit cell density. For rapid fabrication of large parenchymal blocks requiring subsequent vascular seeding, however, volumetric approaches deserve substantially greater attention from the vascularization research community.

7.6. Microfluidic Patterning, Acoustic Bioprinting, and Magnetic Cell Organization

Three additional fabrication technologies have reached proof-of-concept maturity with direct relevance to sub-extrusion-resolution vascular channel formation. Microfluidic-assisted vascular patterning generates endothelializable lumens at 50–200 μm diameter via laminar co-flow of cell-laden and sacrificial streams [65,66]; endothelial monolayer formation in GelMA microfluidic channels within 48 h with barrier function approaching primary endothelium has been demonstrated. Acoustic bioprinting uses focused ultrasound to eject 10–50 μm droplets

from an open reservoir without nozzle contact, eliminating shear stress-driven cell damage intrinsic to piezoelectric inkjet systems [67]. Magnetic cell organization uses iron-oxide nanoparticle-labelled cells positioned by external magnetic field gradients into tubular arrangements before matrix gelation [68], producing perfusable 100–500 μm structures in fibrin matrices within 24 h without any physical contact with cells during assembly [69]. Each approach addresses a specific limitation of conventional bioprinting—resolution, shear damage, and three-dimensional cell positioning respectively, and each is a logical complement to, rather than replacement for, existing macrovascular scaffold strategies.

7.7. AI-Guided Vascular Topology Optimization

Machine learning-assisted generative design has extended computational vascular topology optimization into AI-guided territory. Graph neural network architectures trained on micro-CT datasets of perfused organ specimens predict branching geometries satisfying Murray's Law within arbitrary construct boundaries in seconds, versus hours for conventional finite element optimization [70]. Reinforcement learning frameworks have been applied to maximize perfusion uniformity in simulated hierarchical vascular trees, with reward functions that explicitly penalize regions predicted to experience sub-threshold oxygen partial pressures. The critical bottleneck is the digital manufacturing bridge between optimization output and printer toolpath, mature in industrial additive manufacturing but nascent in bioprinting. As this interface develops, AI-guided topology optimization has the potential to replace channel geometries constrained by designer intuition with networks derived from vascular physiology.

7.8. Lymphatic Vascularization: A Necessary Parallel Challenge

The exclusive focus on blood vessel networks in the bioprinting literature constitutes a gap that weakens the comprehensiveness of the field as a whole. Lymphatic vessels, present in native thick tissues at 10–30 per mm^2 cross-sectional density, perform functions irreplaceable by blood microvasculature: interstitial fluid clearance, immune cell trafficking, and metabolic waste removal [71]. Constructs lacking lymphatic drainage develop interstitial pressures exceeding 5 mmHg within 48 h of implantation in rodent studies, sufficient to compress blood microvessels and negate anastomotic perfusion [72]. iPSC-derived lymphatic endothelial cells form tube-like networks in fibrin matrices with appropriate LYVE-1, PROX1, and VEGFR-3 expression and VEGF-C responsiveness. Their integration into bioprinted constructs alongside blood vascular networks has not been demonstrated at therapeutic scale, but precedent from in vitro co-culture studies supports establishing lymphatic engineering as a parallel, not subsequent, design priority. Constructs that achieve blood vessel anastomosis while neglecting lymphatic drainage risk exchanging one form of vascularization failure for another.

8. A Translational Roadmap Built on Milestones, Not Timelines

Translational roadmaps in tissue engineering have an unfortunate history of optimism. The field has been five to ten years from clinically functional bioprinted organs for most of the last twenty years. We do not intend to repeat that pattern. The roadmap we propose here is organized around specific, measurable milestones that can be evaluated objectively, rather than around calendar timelines that depend on funding trajectories and serendipitous discoveries that cannot be predicted, as set out in **Figure 5**. Phase I (0–3 years) establishes the standardised measurement infrastructure and biological co-culture protocols without which progress cannot be objectively measured. Phase II (3–7 years) targets the demonstration of dual-level (macro + micro) vascular networks in constructs of therapeutic thickness, validated by functional perfusion imaging in large-animal models. Phase III (7–15 years) addresses clinical-scale manufacturing, regulatory engagement, and Phase I trial entry; eight enabling technologies that cross-cut all phases are identified alongside the roadmap. Each milestone represents a genuine state of knowledge, a point at which the community can honestly say that a specific barrier has been addressed, rather than a demonstration that something is possible under carefully optimized conditions.

8.1. Phase I: Build the Measurement Infrastructure First

The single most important near-term investment the bioprinted vascularization field could make is not in a new printing technology or a new bioink chemistry. It is in the development and adoption of shared performance standards that allow results from different laboratories to be compared meaningfully. Specifically: a minimum

functional assessment protocol that every group fabricating vascularized constructs for in vivo testing should apply, including transendothelial resistance ≥15 Ω·cm^2 under 1 dyn/cm^2 shear stress (approximating postcapillary venule conditions), platelet adhesion <10% of area under arterial flow, and oxygen delivery verified by NADH fluorescence lifetime imaging at construct depths beyond 1 mm from any channel surface.

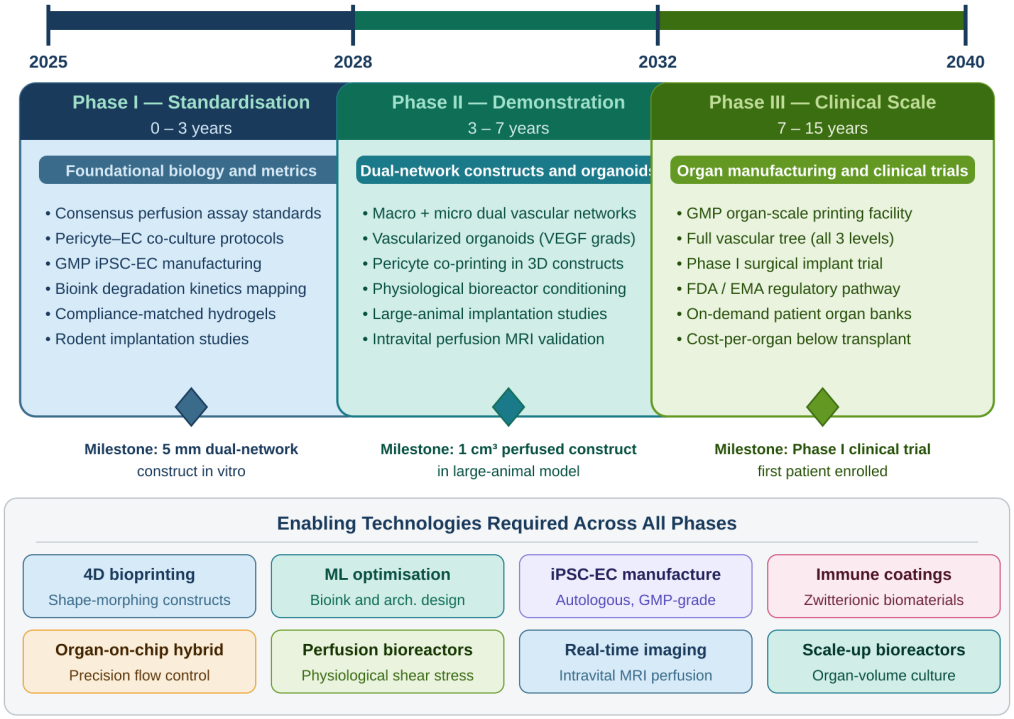

Figure 5. Proposed three-phase translational roadmap for achieving functional in vivo vascularization in bioprinted tissue constructs, structured around demonstrable milestones rather than calendar predictions.

Simultaneously, the biological groundwork for pericyte co-culture must be laid. The field needs protocols specifying: the optimal iPSC-EC:iPSC-pericyte ratio for bioink mixing (our estimate based on native tissue biology is 8:1 to 12:1, but this needs empirical verification in printed constructs); the minimum pericyte density required for endothelial stabilization under culture conditions without exogenous growth factors; and the maximum shear stress that iPSC-EC/pericyte co-cultures can sustain without pericyte detachment. These numbers do not currently exist in the literature in a form applicable to bioprinted constructs.

8.2. Phase II: Prove the Dual-Network Architecture Works In Vivo

The milestone for Phase II is specific: a bioprinted construct of at least 8 mm thickness and 500 mm^3 volume, containing a macrovascular channel network connected to a biologically assembled microvascular bed, demonstrating perfusion by intravital multiphoton microscopy at depths greater than 3 mm from any surface, at 28 days post-implantation in an immunocompetent (not merely immunosuppressed) large-animal model. This milestone is demanding by design. Immunocompetent large-animal models expose constructs to the full immune challenge they will face clinically. Twenty-eight days is sufficient for the initial inflammatory response to resolve and for the durability of anastomosis to be assessed. Perfusion at 3 mm depth verifies that the dual-network architecture is doing what it claims, delivering blood to the construct interior, not merely to its surface.

Reaching this milestone requires parallel advances in at least three areas: a bioink that supports both macrovascular channel integrity over 28 days and microvascular angiogenic sprouting; a pericyte co-culture protocol validated at scale; and a bioreactor conditioning regime that establishes endothelial shear-stress adaptation before implantation. None of these is individually beyond current state-of-the-art. Their simultaneous integration into a single construct protocol is the engineering challenge.

8.3. Phase III: Engage Regulators before the Clinic Engages You

The regulatory pathway for bioprinted vascularized constructs in the major jurisdictions—the United States, European Union, United Kingdom, and China—is not defined, and the absence of that definition is itself a barrier that will delay clinical translation regardless of how well the biology performs. Bioprinted constructs combine features of medical devices (the scaffold), advanced therapy medicinal products (the cells), and potentially biological medicines (secreted growth factors), and no existing regulatory category captures all three simultaneously. The U.S. Food and Drug Administration's (FDA's) Breakthrough Therapy designation and its Regenerative Medicine Advanced Therapy pathway provide mechanisms for accelerated guidance development, and early engagement with these mechanisms—ideally before the first animal studies intended to support a regulatory submission—can reduce the time between positive pre-clinical results and clinical trial authorization by years.

More specifically, bioprinted vascular constructs in the European Union are likely classified as Advanced Therapy Medicinal Products (ATMPs) under Regulation (EC) No 1394/2007, imposing GMP manufacturing requirements, risk-based quality systems, and centralized European Medicines Agency (EMA) authorization. In the United States, the Center for Biologics Evaluation and Research (CBER) has primary jurisdiction under the 351 PHS Act framework; the Regenerative Medicine Advanced Therapy (RMAT) designation enables rolling review and early regulatory interaction. Clinical bioprinting systems will require software validation under 21 CFR Part 11 and IEC 62304. Since cell-containing constructs cannot be terminally sterilized, sterility validation must rely on validated closed-system aseptic manufacturing with environmental monitoring to ISO 14644 Class 5 or better. ISO 13485 quality management certification and ISO 10993 biocompatibility testing are prerequisites in all major jurisdictions. Because bioprinted vascular constructs simultaneously incorporate scaffold devices, cellular components, and biologically active secreted factors, no single existing regulatory category captures the full product; sponsors will need to negotiate a combination product pathway with regulators well before submitting clinical trial applications.

Clinical-scale manufacturing represents the other dimension of Phase III that is chronically underinvested in academic bioprinting research. Printing a 200 mm^3 proof-of-concept construct in a university laboratory and printing a 150,000 mm^3 hepatic lobe under GMP conditions with batch-to-batch consistency and a validated sterility assurance level are operations that differ not just in scale but in kind. The design of bioprinters capable of organ-scale printing in GMP environments, with closed sterile fluidic systems, validated cleaning protocols, environmental monitoring, and electronic batch records, is an engineering project that requires industrial engineering expertise and industrial capital. Academic groups should be partnering with device manufacturers on this challenge now, not after a clinical indication is established.

9. Discussion

Several important recent developments in the field deserve acknowledgement alongside the failure analysis presented in this review. Volumetric bioprinting approaches have advanced considerably since 2022, with demonstrated print times under 30 s for centimetre-scale constructs and improvements in cellular viability attributable to reduced cumulative light exposure [63,64]. AI-assisted vascular network generation, using graph neural networks trained on micro-CT vascular datasets, now enables Murray's Law-compliant network topology within arbitrary construct geometries in under one minute of computation time [70]. Four-dimensional (4D) bioprinting strategies that exploit thermally or biochemically responsive shape-change in printed structures to drive self-assembly of vascular geometries post-printing represent an emerging paradigm that the field is beginning to explore. Decellularized vascular matrix-based systems have demonstrated superior angiogenic support relative to synthetic hydrogels in comparative studies, owing to the retention of native growth factor binding sites and basement membrane proteins; their integration into hierarchical channel fabrication pipelines remains an active area of development. Bioprinted organoid vascularization, the induction of vascular networks within organoid structures that can then be integrated into larger printed architectures, represents a convergence of organoid biology and bioprinting that several groups are pursuing with early promising results. Bioreactor-assisted endothelial maturation studies have confirmed that physiological shear pre-conditioning substantially improves endothelial barrier integrity and reduces thrombotic potential in printed channels, reinforcing the importance of the bioreactor phase in the translational roadmap proposed in Section 8.

Stepping back from the mechanistic analysis, several broader observations emerge that seem worth stating

plainly.

The vascularization crisis is not a problem of insufficient creativity. The literature contains an abundance of creative approaches, coaxial printing, sacrificial templating, FRESH, AV loops, growth factor gradients, self-assembly, organ-on-chip integration, 4D morphing. The challenge is not a deficit of fabrication ideas; rather, it is that the biological complexity of the in vivo environment imposes constraints on channel stability that are not captured by in vitro models. Creative fabrication ideas will likely continue to proliferate; what the field arguably needs most is mechanistic understanding of failure that may help distinguish between approaches that address root causes of in vivo failure and those that primarily improve in vitro appearance without necessarily changing post-implantation outcomes.

The field also needs to be honest about what constitutes evidence of success. A bioprinted construct that maintains patent channels and viable cells in bioreactor culture for four weeks is a noteworthy achievement, but it is not evidence of vascularization in the clinically relevant sense of the term, that is, a construct that establishes perfusion from host circulation and maintains it while integrated into a living patient. The semantic conflation of in vitro perfusion with in vivo vascularization is pervasive in the literature, in grant applications, and in press releases, and it inflates the apparent maturity of the field in ways that mislead funding decisions and set unrealistic expectations for timelines.

Finally, this review was written from a mechanical engineering perspective, and it is worth acknowledging the limits of that perspective. The questions we have identified as most critical—pericyte biology, immune evasion, angiogenic signalling networks, stem cell differentiation fidelity—are fundamentally biological questions that require biological expertise to resolve. The contribution that mechanical engineers and materials scientists can make is to design the physical environment in which that biology occurs: the mechanical properties of the matrix, the geometry of the channel architecture, the flow conditions in the bioreactor, the surface chemistry of the channel wall. Getting those physical parameters right does not guarantee biological success, but getting them wrong guarantees biological failure. That is the scope of what this review has tried to establish.

10. Conclusions

This review has examined the vascularization problem in 3D bioprinting through the lens of failure analysis rather than achievement celebration. The conclusions that emerge from that analysis are the following.

1. The 200 μm oxygen diffusion limit is an inviolable physical constraint, not a modelling assumption. Every fabrication strategy that does not produce a capillary within 200 μm of every cell in a therapeutic construct will fail biologically, regardless of its technical novelty. Current bioprinting cannot directly fabricate capillary-scale networks; biological vasculogenesis must be induced to do so, and the conditions required to induce it within a printed construct of therapeutic thickness have not yet been established.
2. Sacrificial templating is the most mature macrovascular channel fabrication strategy currently available, but it does not solve the microvascular problem. FRESH printing offers higher resolution but has not demonstrated the mechanical stability needed for physiological anastomosis. Coaxial extrusion produces channels but not the branching hierarchy that distribution of flow requires. No individual printing strategy addresses the complete three-level vascular hierarchy.
3. Anastomosis is the least-solved dimension of the vascularization problem. Microsurgical anastomosis of printed channels is mechanically feasible but complicated by compliance mismatch-driven junction failure. Inosculation is biologically real but limited in depth to 1–2 mm. The AV loop produces the best-vascularized constructs in the pre-clinical literature but requires a two-stage surgical procedure. Growth factor-guided angiogenesis produces dysmorphic vessels at the doses needed for centimetre-scale construct penetration.
4. Four mechanistic failure modes—compliance mismatch, degradation-angiogenesis temporal desynchrony, pericyte deficiency, and immune-mediated endothelial destruction—collectively explain why constructs that perform well in bioreactors fail in vivo. Each is addressable, but none is being systematically addressed in most published construct designs. Solving the vascularization crisis requires addressing all four simultaneously, because each is a necessary condition for success, not a factor to be traded against the others.
5. The field lacks the measurement infrastructure needed to distinguish genuine progress from improved in vitro aesthetics. Standardised functional assays—measuring transendothelial resistance, thrombotic potential, and

oxygen delivery at depth—should be adopted as a community standard before further animal experiments are conducted. The cost of these measurements is small; the cost of conducting animal experiments with constructs that would have been filtered out by functional testing is high.

6. Regulatory engagement must begin now, not after pre-clinical success is established. The absence of a defined regulatory pathway for bioprinted vascularized constructs will delay clinical translation independent of biological performance. Proactive engagement with FDA, EMA, and the UK's Medicines and Healthcare products Regulatory Agency (MHRA) through pre-submission meetings, master file submissions, and participation in regulatory science programmes is not a distraction from research; it is a research priority.

The patients waiting for organs that bioprinting might one day provide do not benefit from demonstrations that were beautiful in the laboratory and failed at the bedside. The most respectful thing the field can do for them is to be honest about what has and has not been solved, rigorous in addressing what has not, and realistic about the timeline—not because pessimism is a virtue, but because accurate diagnosis is the necessary first step to effective treatment.

Author Contributions

Conceptualization, I.E.E. and D.C.A.; literature search and analysis, I.E.E., D.C.A., A.E.I., and S.O.; formal analysis and mechanistic synthesis, I.E.E.; investigation and critical appraisal, I.E.E., A.E.I., and S.O.; resources, I.E.E.; visualization, I.E.E., A.E.I., and S.O.; writing—original draft preparation, I.E.E.; writing—review and editing, D.C.A., A.E.I., and S.O.; supervision, I.E.E.; project administration, I.E.E. All authors have read and agreed to the published version of the manuscript.

Funding

This research received no specific grant from any funding agency in the public, commercial, or not-for-profit sectors.

Institutional Review Board Statement

Not applicable. This review did not involve human participants or animals; no new experimental data were generated.

Informed Consent Statement

Not applicable. This review did not involve human participants.

Data Availability Statement

No new data were generated or analysed in support of this research. All data discussed are derived from previously published studies, which are cited in the reference list.

Conflicts of Interest

The authors declare no conflicts of interest.

AI Use Statement

The authors declare that no artificial intelligence (AI) tools were used in the preparation of this manuscript.

Abbreviations

Abbreviation	Full Name
AV loop	Arteriovenous loop
ATMP	Advanced therapy medicinal product
bFGF	Basic fibroblast growth factor
CFD	Computational fluid dynamics
dECM	Decellularized extracellular matrix

EC	Endothelial cell
EMA	European Medicines Agency
FDA	Food and Drug Administration (United States)
FRESH	Freeform Reversible Embedding of Suspended Hydrogels
GelMA	Gelatin methacryloyl
GMP	Good Manufacturing Practice
HUVEC	Human umbilical vein endothelial cell
iPSC	Induced pluripotent stem cell
iPSC-EC	iPSC-derived endothelial cell
MMP	Matrix metalloproteinase
PCL	Polycaprolactone
PDGF	Platelet-derived growth factor
PLGA	Poly(lactic-co-glycolic acid)
RMAT	Regenerative Medicine Advanced Therapy (FDA designation)
TRL	Technology Readiness Level
VEGF	Vascular endothelial growth factor

References

1. Langer, R.; Vacanti, J.P. Tissue engineering. *Science* **1993**, *260*, 920–926.
2. Atala, A.; Bauer, S.B.; Soker, S.; et al. Tissue-engineered autologous bladders for patients needing cystoplasty. *Lancet* **2006**, *367*, 1241–1246.
3. Sun, X.; Ren, W.; Xie, L.; et al. Recent advances in 3D bioprinting of tissues and organs for transplantation and drug screening. *Virtual Phys. Prototyp.* **2024**, *19*, e2384662.
4. Khademhosseini, A.; Langer, R. A decade of progress in tissue engineering. *Nat. Protoc.* **2016**, *11*, 1775–1781.
5. Gao, G.; Cui, X. Three-dimensional bioprinting in tissue engineering and regenerative medicine. *Biotechnol. Lett.* **2016**, *38*, 203–211.
6. Saunders, R.E.; Derby, B. Inkjet printing biomaterials for tissue engineering: bioprinting. *Int. Mater. Rev.* **2014**, *59*, 430–448.
7. Guillotin, B.; Souquet, A.; Catros, S.; et al. Laser-assisted bioprinting of engineered tissue with high cell density and microscale organization. *Biomaterials* **2010**, *31*, 7250–7256.
8. Zhang, Y.S.; Arneri, A.; Bersini, S.; et al. Bioprinting 3D microfibrous scaffolds for engineering endothelialized myocardium and heart-on-a-chip. *Biomaterials* **2016**, *110*, 45–59.
9. Liu, N.; Ye, X.; Yao, B.; et al. Advances in 3D bioprinting technology for cardiac tissue engineering and regeneration. *Bioact. Mater.* **2021**, *6*, 1388–1401.
10. Skylar-Scott, M.A.; Uzel, S.G.M.; Nam, L.L.; et al. Biomanufacturing of organ-specific tissues with high cellular density and embedded vascular channels. *Sci. Adv.* **2019**, *5*, eaaw2459.
11. Kolesky, D.B.; Homan, K.A.; Skylar-Scott, M.A.; et al. Three-dimensional bioprinting of thick vascularized tissues. *Proc. Natl. Acad. Sci. U.S.A.* **2016**, *113*, 3179–3184.
12. Homan, K.A.; Kolesky, D.B.; Skylar-Scott, M.A.; et al. Bioprinting of 3D convoluted renal proximal tubules on perfusable chips. *Sci. Rep.* **2016**, *6*, 34845.
13. Mannoor, M.S.; Jiang, Z.; James, T.; et al. 3D printed bionic ears. *Nano Lett.* **2013**, *13*, 2634–2639.
14. Shen, M.; Wang, L.; Gao, Y.; et al. 3D bioprinting of in situ vascularized tissue engineered bone for repairing large segmental bone defects. *Mater. Today Bio* **2022**, *16*, 100382.
15. Lee, A.; Hudson, A.R.; Shiwarski, D.J.; et al. 3D bioprinting of collagen to rebuild components of the human heart. *Science* **2019**, *365*, 482–487.
16. Mazloomnejad, R.; Babajani, A.; Kasravi, M.; et al. Angiogenesis and re-endothelialization in decellularized scaffolds: Recent advances and current challenges in tissue engineering. *Front. Bioeng. Biotechnol.* **2023**, *11*, 1103727.
17. Akbari, M.; Khademhosseini, A. Tissue bioprinting for biology and medicine. *Cell* **2022**, *185*, 2644–2648.
18. Moroni, L.; Boland, T.; Burdick, J.A.; et al. Biofabrication: A guide to technology and terminology. *Trends Biotechnol.* **2018**, *36*, 384–402.
19. Yeo, M.; Sarkar, A.; Singh, Y.P.; et al. Synergistic coupling between 3D bioprinting and vascularization strategies. *Biofabrication* **2024**, *16*, 012003.
20. Samandari, M.; Mostafavi, A.; Quint, J.; et al. In situ bioprinting: Intraoperative implementation of regenerative medicine. *Trends Biotechnol.* **2022**, *40*, 1229–1247.
21. Datta, P.; Ayan, B.; Ozbolat, I.T. Bioprinting for vascular and vascularized tissue biofabrication. *Acta Biomater.*

2017, *51*, 1–20.
22. Rouwkema, J.; Khademhosseini, A. Vascularization and angiogenesis in tissue engineering: beyond creating static networks. *Trends Biotechnol.* **2016**, *34*, 733–745.
23. Liu, J.; Song, Q.; Yin, W.; et al. Bioactive scaffolds for tissue engineering: A review of decellularized extracellular matrix applications and innovations. *Exploration* **2024**, *4*, 20230078.
24. Grigoryan, B.; Paulsen, S.J.; Corbett, D.C.; et al. Multivascular networks and functional intravascular topologies within biocompatible hydrogels. *Science* **2019**, *364*, 458–464.
25. Taylor, C.A.; Draney, M.T. Experimental and computational methods in cardiovascular fluid mechanics. *Annu. Rev. Fluid Mech.* **2004**, *36*, 197–231.
26. Galie, P.A.; Nguyen, D.H.; Choi, C.K.; et al. Fluid shear stress threshold regulates angiogenic sprouting. *Proc. Natl. Acad. Sci. U.S.A.* **2014**, *111*, 7968–7973.
27. Tocchio, A.; Tamplenizza, M.; Martello, F.; et al. Versatile fabrication of vascularizable scaffolds for large tissue engineering in bioreactor. *Biomaterials* **2015**, *45*, 124–131.
28. Wang, H.; Liu, X.; Gu, Q.; et al. Vascularized organ bioprinting: From strategy to paradigm. *Cell Prolif.* **2023**, *56*, e13453.
29. Kim, J.J.; Cho, D.W. Advanced strategies in 3D bioprinting for vascular tissue engineering and disease modelling using smart bioinks. *Virtual Phys. Prototyp.* **2024**, *19*, e2395470.
30. Lee, S.J.; Jeong, W.; Atala, A. 3D bioprinting for engineered tissue constructs and patient-specific models: Current progress and prospects in clinical applications. *Adv. Mater.* **2024**, *36*, e2408032.
31. Gao, Q.; He, Y.; Fu, J.Z.; et al. Coaxial nozzle-assisted 3D bioprinting with built-in microchannels for nutrients delivery. *Biomaterials* **2015**, *61*, 203–215.
32. Jia, W.; Gungor-Ozkerim, P.S.; Zhang, Y.S.; et al. Direct 3D bioprinting of perfusable vascular constructs using a blend bioink. *Biomaterials* **2016**, *106*, 58–68.
33. Shao, L.; Gao, Q.; Xie, C.; et al. Directly coaxial 3D bioprinting of large-scale vascularized constructs with complex geometry. *Biofabrication* **2020**, *12*, 035014.
34. Miller, J.S.; Stevens, K.R.; Yang, M.T.; et al. Rapid casting of patterned vascular networks for perfusable engineered three-dimensional tissues. *Nat. Mater.* **2012**, *11*, 768–774.
35. Kolesky, D.B.; Truby, R.L.; Gladman, A.S.; et al. 3D bioprinting of vascularized, heterogeneous cell-laden tissue constructs. *Adv. Mater.* **2014**, *26*, 3124–3130.
36. Zhu, W.; Qu, X.; Zhu, J.; et al. Direct 3D bioprinting of prevascularized tissue constructs with complex microarchitecture. *Biomaterials* **2017**, *124*, 106–115.
37. Hinton, T.J.; Jallerat, Q.; Palchesko, R.N.; et al. Three-dimensional printing of complex biological structures by freeform reversible embedding of suspended hydrogels. *Sci. Adv.* **2015**, *1*, e1500758.
38. Ouyang, L.; Highley, C.B.; Sun, W.; et al. A generalizable strategy for the 3D bioprinting of hydrogels from nonviscous photo-crosslinkable inks. *Adv. Mater.* **2017**, *29*, 1604983.
39. Brassard, J.A.; Nikolaev, M.; Hübscher, T.; et al. Recapitulating macro-scale tissue self-organization through organoid bioprinting. *Nat. Mater.* **2021**, *20*, 22–29.
40. Skylar-Scott, M.A.; Huang, J.Y.; Lu, A.; et al. Orthogonally induced differentiation of stem cells for the programmatic patterning of vascularized organoids and bioprinted tissues. *Nat. Biomed. Eng.* **2022**, *6*, 449–462.
41. Levenberg, S.; Rouwkema, J.; Macdonald, M.; et al. Engineering vascularized skeletal muscle tissue. *Nat. Biotechnol.* **2005**, *23*, 879–884.
42. Laschke, M.W.; Harder, Y.; Amon, M.; et al. Angiogenesis in tissue engineering: Breathing life into constructed tissue substitutes. *Tissue Eng.* **2006**, *12*, 2093–2104.
43. Sakaguchi, K.; Shimizu, T.; Horaguchi, S.; et al. In vitro engineering of vascularized tissue surrogates. *Sci. Rep.* **2013**, *3*, 1316.
44. Nguyen, D.H.; Stapleton, S.C.; Yang, M.T.; et al. Biomimetic model to reconstitute angiogenic sprouting morphogenesis in vitro. *Proc. Natl. Acad. Sci. U.S.A.* **2013**, *110*, 6712–6717.
45. Laschke, M.W.; Menger, M.D. Vascularization in tissue engineering: Angiogenesis versus inosculation. *Eur. Surg. Res.* **2012**, *48*, 85–92.
46. Tremblay, P.L.; Hudon, V.; Berthod, F.; et al. Inosculation of tissue-engineered capillaries with the host's vasculature in a reconstructed skin transplanted on mice. *Am. J. Transplant.* **2005**, *5*, 1002–1010.
47. Hudon, V.; Berthod, F.; Black, A.F.; et al. A tissue-engineered endothelialized dermis to study the modulation of angiogenic and angiostatic molecules on capillary-like tube formation in vitro. *Br. J. Dermatol.* **2003**, *148*, 1094–1104.
48. Weigand, A.; Horch, R.E.; Boos, A.M.; et al. The arteriovenous loop: Engineering of axially vascularized tissue.

Eur. Surg. Res. **2018**, *59*, 286–299.
49. Jiang, H.; Li, X.; Chen, T.; et al. Bioprinted vascular tissue: Assessing functions from cellular, tissue to organ levels. *Mater. Today Bio* **2023**, *23*, 100846.
50. Niklason, L.E.; Gao, J.; Abbott, W.M.; et al. Functional arteries grown in vitro. *Science* **1999**, *284*, 489–493.
51. Furdella, K.J.; Higuchi, S.; Behrangzade, A.; et al. In-vivo assessment of a tissue engineered vascular graft computationally optimized for target vessel compliance. *Acta Biomater.* **2021**, *123*, 298–311.
52. Murfee, W.L.; Wagenseil, J.E. Editorial: Putting engineering back in vascular tissue engineering to advance basic science and clinical applications. *Front. Cardiovasc. Med.* **2022**, *9*, 1025465.
53. Shakeel, A.; Corridon, P.R. Mitigating challenges and expanding the future of vascular tissue engineering—are we there yet? *Front. Physiol.* **2023**, *14*, 1079421.
54. Kyriakides, T.R.; Kim, H.J.; Zheng, C.; et al. Foreign body response to synthetic polymer biomaterials and the role of adaptive immunity. *Biomed. Mater.* **2022**, *17*, 022007.
55. Ricklin, D.; Hajishengallis, G.; Yang, K.; et al. Complement: A key system for immune surveillance and homeostasis. *Nat. Immunol.* **2010**, *11*, 785–797.
56. Anderson, J.M.; Rodriguez, A.; Chang, D.T. Foreign body reaction to biomaterials. *Semin. Immunol.* **2008**, *20*, 86–100.
57. Hachim, D.; LoPresti, S.T.; Yates, C.C.; et al. Shifts in macrophage phenotype at the biomaterial interface via IL-4 eluting coatings are associated with improved implant integration. *Biomaterials* **2017**, *112*, 95–107.
58. Takahashi, K.; Yamanaka, S. Induction of pluripotent stem cells from mouse embryonic and adult fibroblast cultures by defined factors. *Cell* **2006**, *126*, 663–676.
59. Bhattacharjee, T.; Zehnder, S.M.; Rowe, K.G.; et al. Writing in the granular gel medium. *Sci. Adv.* **2015**, *1*, e1500655.
60. Baranski, J.D.; Chaturvedi, R.R.; Stevens, K.R.; et al. Geometric control of vascular networks to enhance engineered tissue integration and function. *Proc. Natl. Acad. Sci. U.S.A.* **2013**, *110*, 7586–7591.
61. Shin, J.; Lee, Y.; Li, Z.; et al. Optimized 3D bioprinting technology based on machine learning: A review of recent trends and advances. *Micromachines* **2022**, *13*, 363.
62. Bersini, S.; Gilardi, M.; Arrigoni, C.; et al. Human *in vitro* 3D co-culture model to engineer vascularized bone-mimicking tissues combining computational tools and statistical experimental approach. *Biomaterials* **2016**, *76*, 157–172.
63. Loterie, D.; Delrot, P.; Moser, C. High-resolution tomographic volumetric additive manufacturing. *Nat. Commun.* **2020**, *11*, 852.
64. Bernal, P.N.; Delrot, P.; Loterie, D.; et al. Volumetric bioprinting of complex living-tissue constructs within seconds. *Adv. Mater.* **2019**, *31*, e1904209.
65. Ghorbanian, S.; Qasaimeh, M.A.; Akbari, M.; et al. Microfluidic direct writer with integrated declogging mechanism for fabricating cell-laden hydrogel constructs. *Biomed. Microdevices* **2014**, *16*, 387–395.
66. Colosi, C.; Shin, S.R.; Manoharan, V.; et al. Microfluidic bioprinting of heterogeneous 3D tissue constructs using low-viscosity bioink. *Adv. Mater.* **2016**, *28*, 677–684.
67. Jentsch, S.; Nasehi, R.; Kuckelkorn, C.; et al. Multiscale 3D bioprinting by nozzle-free acoustic droplet ejection. *Small Methods* **2021**, *5*, e2000971.
68. Souza, G.R.; Molina, J.R.; Raphael, R.M.; et al. Three-dimensional tissue culture based on magnetic cell levitation. *Nat. Nanotechnol.* **2010**, *5*, 291–296.
69. Krebs, M.D.; Erb, R.M.; Yellen, B.B.; et al. Formation of ordered cellular structures in suspension via label-free negative magnetophoresis. *Nano Lett.* **2009**, *9*, 1812–1817.
70. Hague, J.P. Simultaneous self-organization of arterial and venous networks driven by the physics of global power optimization. *arXiv preprint* **2023**, *arXiv.2308.02700*. [CrossRef]
71. Alitalo, K. The lymphatic vasculature in disease. *Nat. Med.* **2011**, *17*, 1371–1380.
72. Kolarzyk, A.M.; Wong, G.; Lee, E. Lymphatic tissue and organ engineering for *in vitro* modeling and *in vivo* regeneration. *Cold Spring Harb. Perspect. Med.* **2022**, *12*, a041169.